NASA Technical Paper 2913

1989

Evaluation of the Ride Quality of a Light Twin-Engine Airplane by Means of a Ride Quality Meter

Eric C. Stewart
Langley Research Center
Hampton, Virginia

NASA
National Aeronautics and Space Administration
Office of Management
Scientific and Technical Information Division

Summary

A ride quality meter has been used to establish the baseline ride quality of a light twin-engine airplane planned for use as a test bed for an experimental gust alleviation system. The ride quality meter provides estimates of passenger ride discomfort as a function of cabin noise and vibration (acceleration) in five axes (yaw axis omitted). According to the ride quality meter, in smooth air the cabin noise was the dominant source of passenger discomfort. In moderately turbulent air with approximately the same cabin noise level, the vertical and lateral vibrations (accelerations) were the dominant sources of passenger discomfort, but the total discomfort was approximately the same as that for the smooth-air condition. The researcher's subjective opinion, however, is that the total ride discomfort was much worse in the moderate turbulence than it was in the smooth air. The discrepancy is explained by the lack of measurement of the low-frequency accelerations by the ride quality meter.

Introduction

General aviation airplanes have a reputation for poor ride quality. One of the primary complaints is that general aviation airplanes have a rough ride, especially in turbulent air. In order to address the apparent need for improvement in this area, NASA initiated a research program through a grant to the University of Kansas to develop and test an experimental gust alleviation system (ref. 1). However, there is a limited data base for modern general aviation airplanes from which to design this system. For example, there are very few experimental data to indicate exactly which motion parameters and which frequency ranges need to be controlled in small airplanes to provide the most improvement in ride comfort as perceived by a representative sample of passengers. That is, there are few data for small airplanes to indicate whether both a longitudinal and a lateral gust alleviation system are necessary. Recent tests of an experimental gust alleviation system on a commuter airplane (ref. 2) have also indicated that although the gust alleviation system effectively reduced the low-frequency accelerations, "...the sensitivity of the human body to vertical accelerations of 4.0 to 8.0 Hz and more is higher than expected." In addition, there are many other important nonmotion factors such as noise that affect the overall ride quality (ref. 3). There is no guarantee that a perfectly gust-alleviated general aviation airplane, for example, would be significantly more acceptable to a large segment of the general population without additional improvements in other areas. There are no data for general aviation airplanes to define exactly how important these other, nonmotion, factors are and what their relationship, and interaction, is with the accelerations. Finally, there are also very few experimental data which define the frequency content of the response of modern general aviation airplanes to turbulence. The frequency content is vital for adequately specifying the requirements for the sensors and actuators that could be used in such a gust alleviation system. Experimental flight data are needed to supplement and validate theoretical calculations of frequency content such as those based on the Dryden gust spectrum and linear airplane response models.

In an effort to provide some of these needed data, a flight test study was conducted with the airplane planned for use in the NASA/University of Kansas gust alleviation program. A new Langley-developed ride quality meter was used to document the baseline ride quality for this light, twin-engine general aviation airplane. The new meter provides real-time estimates of the ride quality as a function of acceleration levels and cabin noise as perceived by "naive" passengers. The ride quality meter automatically ranks the individual contributions to the overall ride quality of five axes of acceleration and of six different octave bands of cabin noise. This meter had been used previously in a variety of air and land vehicles, but it had never before been applied to a general aviation airplane. Therefore, these tests also served to evaluate the applicability of the meter to general aviation airplanes and to determine its suitability for future use in documenting the effectiveness of the planned gust alleviation system.

The present measurements were made during 13 flights over a period of 3 months. The ride quality was documented with the ride quality meter for all phases of flight, from taxiing for takeoff to landing. The ride quality for the in-flight phase of operation was documented for estimated levels of turbulence from smooth to moderate turbulence. By comparing the meter-predicted ride quality in smooth-air conditions with that in turbulence, estimates of the maximum improvement in ride quality that could be obtained with a perfect gust alleviation system without changing the cabin noise levels were obtained. The meter estimates of the ride quality were also compared with the subjective opinion of the flight crew. In addition, time histories and rms power spectra of the airplane accelerations in turbulence were obtained.

Symbols and Abbreviations

dB(A)	A-weighted sound pressure level in decibels

DISC	passenger discomfort index units
DNOISE	combined noise discomfort index, DISC units
DTOTAL	total discomfort index, DISC units
DVIB	acceleration discomfort index, DISC units
g	acceleration due to gravity, 32.2 ft/sec^2
h	altitude, ft
IAS	indicated airspeed, knots
MAP	engine manifold pressure, inches of mercury (Hg)
N	engine speed, rpm
rms	root mean square value
rpm	revolutions per minute
RQM	ride quality meter
Δa_x	longitudinal acceleration after filtering, g units positive toward nose
Δa_y	lateral acceleration after filtering, g units positive out right wing
Δa_z	vertical acceleration after filtering, g units positive down
$\Delta\ddot{\theta}$	pitch acceleration after filtering, rad/sec^2, positive nose up
$\Delta\ddot{\phi}$	roll acceleration after filtering, rad/sec^2, positive right wing down

Description of Test Apparatus

Ride Quality Meter

The ride quality meter (RQM) system consists of three separate components: the computer-printer package, the accelerometer package, and a sound level meter and microphone, as shown in figure 1. The RQM system was designed for quick installation in a wide variety of vehicles. Ordinarily the RQM computer-printer package is placed in an empty seat with the accelerometer package on the floor in front of or beneath the seat. In the present application, however, each piece was rigidly attached to the instrument pallet shown in figure 1. The computer-printer package and the accelerometer package required a 12-V dc (5-A) power source, and the sound level meter operated on internal dry cell batteries. The total system weight was about 40 lb.

Time histories of the accelerometer outputs were recorded on analog tape. The tape recordings were processed after the flights on a spectral analyzer for a more detailed description of the aircraft motions.

Background. The RQM was developed to provide a general and comprehensive empirical estimate of passenger ride comfort as a function of vehicle vibration (acceleration) and interior noise. The accelerations are referred to as vibrations in reference 4 because frequencies ranging from a low of 0.5 or 1.0 Hz up to a high of 10 Hz (30 Hz in the vertical axis) were used in the development of the ride comfort model. However, since frequencies as low as 0.1 Hz are considered in this report, the more general term acceleration will be used in all cases. The NASA ride comfort algorithm was developed in a research program that obtained subjective comfort ratings from more than 3000 people who were exposed to controlled combinations of noise and acceleration in the Passenger Ride Quality Apparatus at the NASA Langley Research Center. Although the apparatus was capable of producing oscillatory accelerations in all three linear axes (longitudinal, lateral, and vertical), it could produce angular accelerations in only the pitch and roll axes (no yawing acceleration). The resulting model does not, therefore, account for yawing motions. The basic principle of operation of the model is to transform the individual components of the noise and the accelerations into subjective discomfort indexes with common units and then combine these subjective indexes to produce a single total discomfort index typifying naive passenger acceptance of the environment (see ref. 5).

The total and intermediate discomfort indexes are directly proportional to subjective discomfort and have ratio scale properties. For example, a discomfort index of 4.0 represents twice the discomfort associated with a discomfort index of 2.0, and a discomfort index of 0.5 represents one-half the discomfort represented by an index of 1.0. The discomfort indexes are typically used to indicate relative values of discomfort in a given ride environment, although it is possible to assign absolute meanings to the discomfort scale. The relationship between the ride comfort index and the percentage of uncomfortable passengers is established by conducting "calibration" tests within the vehicle of interest. These tests are necessary because subjective criteria for assigning absolute discomfort within a given vehicle depend to some extent on the context of the ride environment being

considered. This calibration procedure is illustrated in reference 6 for a group of helicopter pilots in simulated helicopter environments. Since the absolute scale for the present airplane was not established, the results of reference 6 were used to give some perspective to the discomfort indexes measured in the present study.

Ride comfort algorithms. A complete description of the ride comfort algorithms is given in reference 7. The basic elements of the ride comfort algorithm are shown in figure 2.

The signals output by the linear and angular accelerometer package are first processed by the single-axis algorithms. These algorithms use passive filters to provide a frequency weighting to the accelerometer signals that reflects the acceleration-frequency dependence of human discomfort for each axis. These weighting functions are different for each axis of motion and are presented later. The weighted signals are then squared and time-averaged to produce weighted rms accelerations. The last step in the single-axis algorithms is to use the weighted rms accelerations in empirically determined linear equations to calculate the single-axis discomfort indexes, DVERT, etc.

The single-axis discomfort indexes are then applied to the combined-axes algorithms to calculate the total discomfort caused by the accelerations, DVIB. These algorithms rank the individual acceleration discomfort indexes and then calculate a vector sum of the ranked indexes to determine the total acceleration discomfort index; see reference 7 for the exact calculations. The total acceleration discomfort, DVIB, is also used in calculating the noise discomfort as indicated by the cross-feed path in figure 2 and as explained below.

The noise discomfort contributions are computed for noises within six octave bands having center frequencies of 63, 125, 250, 500, 1000, and 2000 Hz. The A-weighted sound pressure levels between 65 dB(A) and 100 dB(A) within each of the six octave bands are weighted on the basis of passenger discomfort sensitivity in the noise octave band algorithm. A key feature of the algorithm is that the discomfort caused by noise depends on the level of acceleration discomfort present in the ride environment. This dependence is indicated by the cross-feed path from the acceleration output, DVIB, to the noise octave band algorithm in figure 2. For a given noise level, the computed noise discomfort index (restricted to positive values) is linearly reduced by the acceleration discomfort index, DVIB. This physically means that passengers usually are less concerned with a given level of noise when the acceleration level is high (rough ride) than they are when the acceleration level is low (smooth ride).

The individual noise discomfort indexes, D63, etc., are next applied to the noise combined octave algorithm, which calculates the total noise discomfort index, DNOISE, using a summation procedure on the ranked indexes. The final step in the calculations is to sum the discomfort caused by the acceleration and the discomfort caused by the noise to produce the total discomfort, DTOTAL.

Meter operation. The operation of the RQM is very simple. With the power turned on, the researcher activates the data-taking function when an interesting ride condition arises. The meter then automatically samples the acceleration and noise data and performs the calculations. After about 20 sec the meter begins printing the noise and acceleration levels and the various discomfort indexes. The printing cycle lasts about an additional 30 sec for a total cycle time of about 50 sec. The process will then be automatically repeated unless terminated by the researcher.

The tape recorder was operated independently of the RQM, but was generally turned on whenever the RQM was taking, but not printing, data. The average lengths of the recordings were, therefore, about 30 to 40 sec, which made it possible to analyze frequencies down to about 0.1 Hz, assuming four data samples per cycle are required to accurately describe a given frequency.

Airplane

Physical characteristics. The airplane used in the present tests (see fig. 3) was an eight-passenger, low-wing, light twin-engine configuration that is used extensively in commuter operations. The overall physical dimensions of the airplane are given in the three-view drawing shown in figure 4. The airplane has a maximum takeoff weight of 6300 lb and is powered by two 300-hp turbocharged piston engines. Operations are ordinarily limited to altitudes below 10 000 ft because the airplane cabin cannot be pressurized. A summary of some of the primary airplane characteristics is given in table I.

Ride quality meter installation. The RQM components were rigidly attached to an instrument pallet and installed on the seat rails in place of the seat immediately behind the pilot's seat. (See fig. 5.) A separate power supply mounted on the pallet was used to convert the 28 V of the basic electrical system of the airplane to the 12 V required by the RQM. The research engineer sat immediately behind the copilot's seat and operated the RQM during flight. Seats were not installed in the aft cabin for the tests,

but the airplane was otherwise in a configuration similar to that which would be used in commuter operations; that is, carpeting and other standard sound absorbing trim were in place.

Flight Test Program

Typically the airplane was flown with a takeoff weight of approximately 5750 lb and was flown for 1 to 2 hr, during which 180 to 360 lb of fuel were consumed. The crew consisted of the pilot, the crew chief, and the research engineer. With this loading the center of gravity was in a forward location at 21.6 percent of the mean aerodynamic chord.

A summary of the flight conditions used in the present study is given in table II. These conditions are representative of typical operations of this airplane from takeoff to landing. Extensive additional data were recorded in flight conditions approximating the cruise condition in table II because the largest percentage of commuter flight time is in the cruise condition. Most of these additional measurements were made in order to document the ride quality in turbulent flight conditions. In an attempt to find the most turbulent conditions, slightly different altitudes and airspeeds from those shown in table II for the cruise condition were used. For example, flights downwind of the crest of the Blue Ridge Mountains of Virginia (altitudes 3000 to 4500 ft) were flown.

Discussion of Results

Characteristic RQM Results

Typical RQM printout. A copy of an RQM printout for a typical smooth-air flight condition is shown in table III. The top section of the printout contains the octave-band noise levels and their discomfort indexes, and the bottom section contains the weighted rms acceleration levels and their discomfort indexes. Printed between the two sections are the total discomfort index, DTOTAL, the combined noise index, DNOISE, and the combined acceleration index, DVIB. The total ride discomfort index was about 5.1, with 4.2 of the total due to noise and 0.9 due to acceleration. (For comparison, the RQM reading with the airplane parked in the hangar without the engines running was 0.1, which was due entirely to the electrical noise on the accelerometer signals. A typical reading in an automobile travelling 45 miles per hour on a two-lane road with the windows up is 2.0 to 3.0). The printout indicates that the 125-Hz octave band was the primary source of noise discomfort (3.6), and the vertical and roll accelerations were the primary sources of acceleration discomfort (0.6 and 0.3, respectively). The noise level at 125 Hz was almost 94 dB(A), and the weighted rms vertical and roll accelerations were $0.01g$ and 0.11 rad/sec^2, respectively. It should be noted that neither the noise nor the acceleration discomfort index is a simple sum of the individual components. As explained in the section "Ride comfort algorithms," the algorithm reflects the passenger's preoccupation with the most uncomfortable stimuli and the disregard of less uncomfortable stimuli.

The fact that more than 80 percent of the total ride discomfort index in smooth air was due to noise was not surprising. The noise level in this airplane was high and conversation difficult. On the other hand, the ride, though not qualitatively as smooth as that of a big automobile on a good road, seemed very acceptable to the crew.

Repeatability of measurements. The discomfort indexes for four consecutive measurements in cruise are presented in figure 6. The turbulence level was judged by the crew to be "light" but was, of course, not exactly the same for all four measurements. The four measured indexes were repeatable to within about 0.3 unit of the ride comfort scale. This was typical of the repeatability experienced at other flight conditions.

Sensitivity to airspeed and engine power. The effect of airspeed on the acceleration, noise, and total discomfort indexes is shown in figure 7. Note that the noise discomfort index is equal to the difference between the total discomfort index and the acceleration discomfort index. As the airspeed was increased at a constant power setting (the vertical speed was allowed to vary as the airspeed was changed), the total discomfort index increased. Almost the entire increase was due to the increasing noise level, although the acceleration component of discomfort also increased slightly.

The effect of engine power on the acceleration, noise, and total discomfort indexes is shown in figure 8. At a constant airspeed of 140 knots and a propeller speed of 2300 rpm, the total discomfort index increased with increasing manifold pressure (power level). Again the data show that almost all the increase was due to the cabin noise, since the acceleration was very low in the smooth-air conditions in which these data were taken.

In summary, there was a significant variation in the ride quality index with both airspeed and engine power. Most of the variation was due to changes in the cabin noise level. Thus, when comparing the noise discomfort indexes for different airplane configurations, it is important to use the same airspeed and power level.

Basic Ride Quality

Ride quality in different phases of flight. The ride discomfort indexes in smooth air for the eight different phases of a typical flight are shown in figure 9. As mentioned earlier, the study in reference 6 determined the relationship between the percentage of helicopter pilots who found a given ride environment uncomfortable and the corresponding discomfort indexes calculated by the ride quality meter. This scale is shown on the right of figure 9 for comparison. The reader is cautioned, however, that the validity of the percentage scale for the present investigation has not been established.

In the taxi phase of the flight, the acceleration was the dominant source of ride discomfort, although the overall ride comfort was relatively good compared with that in flight. The acceleration was probably caused by rolling on the taxiway and not by the operation of the engines. The cabin noise during taxiing was low because engine power was very low.

During engine run-up, the acceleration discomfort was reduced even though the high engine speeds caused the airplane to vibrate noticeably. Evidently this increased engine vibration was more than offset by the absence of accelerations due to rolling on the taxiway because the airplane was stationary during engine run-up. However, noise from the engines and propellers was greatly increased, and the resulting total discomfort index was essentially unchanged.

During the takeoff roll, the acceleration component of discomfort increased to a level about one-third higher than during taxi. This was probably due to the higher average rolling speed on the runway. The discomfort index caused by the increased cabin noise was less than that during the engine run-up because of the effect of the increased accelerations and not because of a lower noise level. As explained earlier, at a fixed noise level the ride comfort algorithm produces a lower noise discomfort index as the acceleration level increases. This algorithm reflects the passengers' preoccupation with the acceleration stimuli at high acceleration levels. In other words, the acceleration effectively masks the discomfort due to the noise.

During the in-flight phases, the acceleration discomfort decreased to relatively small values because of the smooth-air conditions, but the noise discomfort contribution increased to large values. This is because the "effective masking" of the noise discomfort by large accelerations was absent. Even though the flight acceleration levels were low, the total discomfort showed little or no improvement compared with the high-acceleration condition of the takeoff roll. In fact, over 90 percent of the helicopter pilots in reference 6 would still be uncomfortable during such flight even though the ride was very smooth.

During the final phase of flight, the landing roll, discomfort caused by accelerations again increased to the level present in the takeoff roll. However, since the engine power was now at a very low level, the discomfort caused by the noise was zero.

In summary, except for the taxi and engine run-up phases of flight, the RQM algorithm predicts a relatively constant total passenger discomfort. However, the passengers would perceive the discomfort as coming from different sources (either noise or acceleration) for the different phases of flight. In addition, since the total discomfort was high in the low acceleration, smooth-air flight condition, ride-smoothing technology by itself as described in reference 1 may not be sufficient to improve the overall ride environment. Both ride smoothing and noise reduction treatments may be required.

Cabin noise analysis. The individual discomfort indexes for the six octave bands contained in the total noise discomfort index for the cruise flight condition of figure 9 are presented in figure 10. Because these individual indexes are not corrected for the influence of the acceleration, they cannot be directly compared with the total, acceleration-corrected, noise index in figure 9. In other words, the indexes in figure 10 represent noise discomfort with acceleration assumed to be zero. The value of the measured A-weighted sound pressure level is also presented for each octave band. The data in figure 10 indicate the primary source of noise discomfort was the 125-Hz octave band. The propeller blade passing frequency for this condition was 115 Hz, indicating that the propulsion system is the source of most of the ride discomfort. Thus, the RQM provides a useful capability for locating the areas for productive ride quality improvements.

Acceleration analysis. The individual axis contributions to the total acceleration discomfort index for the cruise flight condition in figure 9 are presented in figure 11. Also shown are the weighted rms accelerations associated with the individual discomfort indexes. These data indicate that the vertical and lateral axes were the dominant sources of acceleration discomfort, although the magnitude of the indexes was small compared with the noise discomfort indexes. The acceleration discomfort becomes significant in cruise only in turbulent air as shown in the next section.

Ride Quality in Turbulence

Ride comfort measurements during cruise for four flights in different levels of turbulence are shown in figure 12. The designations "smooth," "very light,"

"light," and "moderate" are based on the subjective judgment of the researcher since no direct, quantitative measurement of atmospheric turbulence was made. The relative contribution of acceleration to total discomfort increased until for the moderate turbulence condition the accelerations accounted for all the discomfort. However, as the turbulence level increased, the total discomfort remained relatively constant. It was the judgment of the crew that the ride was much more uncomfortable for the moderate turbulence level than it was for the smooth-air condition because they were being severely bounced around in their seats. The RQM, therefore, correctly identified the source of the discomfort for moderate turbulence, but the total discomfort index did not accurately reflect the actual ride comfort.

There are two factors that may account for the difference between crew perception and RQM estimates of total ride discomfort. First, and most important, the RQM does not respond to vertical and lateral accelerations having frequency content below 1.0 Hz. This is discussed later when the unweighted frequency response data are presented. Second, a slight anomaly was discovered in the ride comfort algorithm for high noise levels and moderate acceleration levels such as those present in these tests. As stated earlier, at a constant noise level, the noise discomfort index was linearly reduced as the acceleration discomfort index increased. At noise levels above about 85 dB(A) it was discovered that the magnitude of this reduction was slightly greater than the increase in the acceleration discomfort index. For example, for the cabin noise levels present in the moderate turbulence condition, an increase in the acceleration discomfort index DVIB of 1.000 discomfort unit would cause a corresponding decrease in the noise index of 1.005 discomfort units. Since the total discomfort index is the sum of the noise and acceleration discomfort indexes, the total discomfort index would be decreased by 0.005 unit for each 1.000 discomfort unit increase in the acceleration discomfort index. This anomaly occurs only for low-to-moderate acceleration levels because negative values of the noise discomfort index are excluded. Thus, after increasing acceleration levels have reduced the noise discomfort index to zero, the total discomfort index is equal to (and increases on a one-to-one basis with) the acceleration discomfort index.

Although theoretically there can be antagonistic interactions such as this to multiple stimuli, the original data from which this algorithm was developed always showed increasing total discomfort as the acceleration increased. In any case, this anomaly is a second order effect compared with the lack of response of the RQM to the lower acceleration frequencies. The latter effect is probably largely responsible for the disagreement between the crew's perception of ride discomfort and the total ride comfort index in different levels of turbulence.

Cabin noise discomfort analysis. The components of the noise discomfort index during cruise in moderate turbulence are presented in figure 13. The indexes presented in figure 13 are for a theoretically acceleration-free environment and are presented in this manner for comparison with figure 10. A comparison of these two figures indicates that the noise level within the four highest octave bands in the moderate turbulence was slightly higher than that in the smooth air. However, the data in figure 12 showed that the noise discomfort was zero in the moderately turbulent air, whereas the noise discomfort in the smooth air was large. This result again reflects the basic phenomenon that naive passengers become less concerned with noise as the acceleration level increases.

Acceleration discomfort analysis. The discomfort components for each axis of motion during cruise in moderate turbulence are shown in figure 14. As expected, the magnitudes of the acceleration components are much larger in turbulence than those presented in figure 11 for smooth air. In addition, the lateral acceleration discomfort in turbulence is almost as large as the vertical acceleration discomfort. An explanation of this result will be discussed in the next section. These RQM data indicate that the lateral acceleration needs to be alleviated as well as the vertical acceleration if a gust alleviation system is to produce significant improvement in ride quality.

Airplane Response to Turbulence

Acceleration time histories. It is useful to examine the time histories of the accelerations in order to understand some of the previous results and in order to document motions of this airplane in turbulence. Time histories of the accelerations during cruise in the moderate turbulence condition are presented in figure 15. The rms level for each filtered acceleration is also shown in the figure. The accelerometer data were passed through a constant amplitude notch filter with a lower cutoff frequency of 0.1 Hz and an upper cutoff frequency of 12.0 Hz. The lower cutoff was used to remove the bias on Δa_z due to the acceleration of gravity, and the upper cutoff frequency was used to remove large acceleration components at 19 and 38 Hz. These high-frequency components were removed because they masked the more interesting lower frequency components when plotted at the time scale used in figure 15. The RQM also removed these components except for the 19-Hz component of

the vertical acceleration. This frequency, however, was not weighted as heavily as the lower frequencies by the RQM.

The longitudinal acceleration Δa_x was relatively small, whereas the lateral acceleration Δa_y and the vertical acceleration Δa_z had peak values of about $0.24g$ and $0.60g$, respectively. It is interesting to compare the rms values of all three accelerations with the RQM-weighted rms values in figure 14. For example, although the unweighted rms lateral acceleration was only 39 percent as large as the unweighted rms vertical acceleration in figure 15, its RQM-weighted value in figure 14 was over 70 percent as large. The discomfort index for the lateral acceleration was about 82 percent as large as the vertical acceleration index because the linear equation relating the weighted rms lateral acceleration to discomfort has slightly larger constants than does the corresponding equation for the vertical acceleration (ref. 7).

The lateral acceleration had a large low-frequency (period of about 2 sec) oscillation which was probably due to the Dutch roll mode. Superimposed on this oscillation were much smaller amplitude, random high-frequency accelerations which were probably due to the direct effects of the turbulence. The Dutch roll oscillation could probably have been effectively suppressed by the yaw damper, but the yaw damper was not engaged during this particular run. The effectiveness of the yaw damper in reducing airplane response to turbulence was not evaluated.

The lateral acceleration was probably due to both the side force from an oscillatory sideslip and the induced linear acceleration from the yawing motion because there was a 2-ft accelerometer package offset from the center of gravity of the airplane. The exact contribution from each of these sources cannot be determined without more extensive measurements. However, for the present accelerometer location a simple one-degree-of-freedom calculation using the side-force characteristics in reference 8 showed that the side force due to sideslip is approximately 3 times as powerful as the yawing motion in producing a given acceleration. Thus, if the accelerometer package had been exactly at the center of gravity, the measured lateral acceleration would have been only 25 percent smaller than presently measured.

The vertical acceleration had much sharper peaks than the lateral acceleration. Direct effects of gusts were much more important because of the larger force-producing capability of the wing as compared with the side of the airplane. The short period mode was much more heavily damped than the Dutch roll mode and thus produced no dominant resonant oscillation.

The pitch and roll accelerations, $\Delta\ddot{\theta}$ and $\Delta\ddot{\phi}$, respectively, contain a broad band of high-frequency, large-amplitude accelerations. There is some evidence of lower frequency motions, especially in the roll acceleration, but most of the acceleration seems to be structural in origin. The structural accelerations are amplified by the turbulence, as will be shown in the following spectral analysis.

Acceleration spectral analysis. The unweighted rms accelerations in the frequency range from 0.125 to 10 Hz for cruise in the very light and moderate turbulence conditions are presented in figures 16 through 20. Also included in the figures are the weighting functions (filters) used in the RQM. As mentioned earlier, these weighting functions reflect human comfort sensitivity to whole-body acceleration in each axis.

The longitudinal acceleration levels were relatively small, and the rms longitudinal acceleration spectra are shown in figure 16 for completeness. The lateral acceleration rms spectra are given in figure 17. These spectra are of more interest since the moderate turbulence spectrum shows a very sharp spectral peak at about 0.5 Hz, which is below the lower limit of 1.0 Hz measured by the RQM. This peak is probably due to the Dutch roll (rigid body) mode of the airplane. According to the theoretical calculations in reference 8, the Dutch roll mode has a natural frequency of 0.4 Hz and a damping ratio of 0.08. As discussed earlier, extension of the RQM frequency range to include the Dutch roll peak would likely have resulted in higher discomfort values for the lateral axis.

The vertical acceleration spectrum for moderate turbulence (see fig. 18) has two peaks at frequencies below 1.0 Hz. The theoretical short period mode had a natural frequency of 0.7 Hz and a damping ratio of 0.9. Because the RQM did not respond to vertical acceleration frequencies below 1.0 Hz, this peak, like the one for the lateral acceleration, was largely ignored by the RQM. These low-frequency peaks were probably responsible for the previously discussed discrepancy between the total ride comfort reading and the crew's subjective opinion of the total ride comfort in the moderate turbulence conditions. A second low-frequency peak in the RQM weighting functions, as suggested in reference 9, for both the lateral and vertical axes at the lower frequencies might be appropriate, but establishing such functions was beyond the scope of the present study. An airplane with a gust alleviation system would be an ideal test bed for establishing these low-frequency weighting functions. That is, low-frequency airplane responses to turbulent conditions could be routinely simulated in smooth air by using the flaps to generate the

appropriate accelerations. Test subjects could then evaluate the ride comfort as in the previous development tests for the RQM, and the low-frequency weighting functions could be determined.

The rms pitching and rolling accelerations (figs. 19 and 20) exhibited no dominant low-frequency peaks and the acceleration levels in moderate turbulence were only about twice those in smooth air. The higher frequencies were more dominant than those for the linear accelerations and were possibly due to structural accelerations of the instrument pallet. However, their magnitudes were also small, and they contributed very little to the overall discomfort index. In the more general case, rigid body angular motions can be important to ride discomfort because they can produce significant linear accelerations at locations removed from the center of gravity. This is especially evident in improperly designed gust-alleviated airplanes, as noted in reference 10.

These power spectral data provide insight for establishing specifications for sensors and actuators for a gust alleviation system for this airplane. The data in figure 18 indicate that actuators with a frequency response of at least 4 Hz are necessary to alleviate the bulk of the vertical gusts. On the other hand, the data in figure 17 indicate that a much slower actuator might be used to alleviate the lateral gusts. In fact, a conventional yaw damper might suffice for the lateral gust alleviation system.

Additional Observations

Other important stimuli not measured by the RQM can affect ride comfort. Cabin temperature and pressure were two obvious stimuli that detracted from ride comfort during the present tests. Others that were more difficult to assess included seating arrangements, visual cues, and ventilation. It would be highly desirable to include these as inputs to a universal ride quality meter. The present RQM assumes that these factors are held constant at acceptable levels since the development data were taken in an airline cabin environment in a ground-based facility. The RQM does provide useful data for developing ride quality augmentation technology as long as its limitations are kept in mind. The present flight tests provide initial information for modifying the weightings of the RQM and extending its frequency range to make it more applicable to actual flight conditions in a turbulent atmosphere.

Concluding Remarks

A new ride quality meter (RQM) has been used to document the ride quality of a light twin-engine airplane. The meter provides real-time quantitative estimates of ride discomfort as perceived by naive passengers as a function of linear and angular vibrations (accelerations) and cabin noise levels. The meter provides not only estimates of the total discomfort but also a ranking (in common units) of the contributions of the individual axes of acceleration and octave bands of noise to the total ride discomfort. The meter indicated a relatively high level of passenger discomfort in all phases of flight from taxi, through flight, to landing. However, the passengers would perceive the source of discomfort as being either noise or acceleration depending on the particular phase of flight.

For the in-flight phases of flight in smooth air, the meter indicated that the total discomfort was relatively high and that the cabin noise produced much more discomfort than the acceleration levels. Thus, a perfectly gust-alleviated airplane that would correspond to this smooth-air condition would have a relatively high discomfort level. In order to appeal to a large segment of the general population, noise treatments as well as gust alleviation seem to be necessary. The meter indicated that the octave band (125-Hz center frequency) containing the propeller blade passing frequency was the dominant source of noise discomfort in this airplane.

In moderate turbulence the meter indicated that the accelerations were the dominant source of discomfort and that the noise discomfort was effectively zero because of the masking effect of the accelerations. In addition, the discomfort due to the vertical acceleration was only slightly larger than the discomfort due to the lateral acceleration. Thus, a gust alleviation system probably needs to alleviate both types of accelerations. Since the vertical acceleration contained significantly higher frequencies than did the lateral acceleration, the vertical gust alleviation system would require faster acting sensors and actuators (up to 4.0 Hz).

The total discomfort index (the sum of the noise and acceleration discomfort indexes) was practically the same in smooth air as it was in moderately turbulent air. This result did not agree with the research crew's subjective judgment that the turbulent condition was much more uncomfortable than the smooth-air condition. This disagreement was probably due to the fact that the RQM did not respond to vertical or lateral accelerations below 1.0 Hz and the airplane accelerations were large in this frequency range. A second, less important, reason for the disagreement was a slight anomaly in the RQM algorithm for high noise levels and moderate acceleration levels. For these conditions the masking effect of the accelerations on the noise discomfort was slightly overestimated.

The RQM, while giving very useful indications of ride quality, could be improved for general aviation applications. The greatest improvement for analyzing the ride of airplanes in turbulent air would be to extend the frequency range to below the rigid body frequencies of the airplane. This extension would probably require a flight-based data base rather than the ground-based data base that the RQM is presently utilizing. An airplane with a gust alleviation system would be an ideal test bed for such a study. The RQM reading also does not reflect other parameters that may be important in general aviation airplanes. Cabin pressure, cabin temperature, ventilation, and visual cues are other parameters that would probably be needed in a general-aviation-oriented RQM.

NASA Langley Research Center
Hampton, VA 23665-5225
April 25, 1989

References

1. Suikat, Reiner; Donaldson, Kent; and Downing, David R.: An Analysis of a Candidate Control Algorithm for a Ride Quality Augmentation System. AIAA-87-2936, Sept. 1987.
2. Max, Heinz: Results of Technology Programs for General Aviation Aircraft at Dornier. *Flight Testing—Evolution and Revolution, Society of Flight Test Engineers 16th Annual Symposium Proceedings,* 1985, pp. 3.6-1–3.6-12.
3. Conner, D. William: Nonmotion Factors Which Can Affect Ride Quality. *1975 Ride Quality Symposium,* NASA TM X-3295, DOT-TSC-OST-75-40, 1975, pp. 87–96.
4. Wood, John J.; and Leatherwood, Jack D.: A New Ride Quality Meter. *Surface Vehicle Noise and Vibration Conference,* P-161, Soc. of Automotive Engineers, May 1985, pp. 177–183. (Available as SAE Tech. Paper Ser. 850981.)
5. Leatherwood, Jack D.; Dempsey, Thomas K.; and Clevenson, Sherman A.: A Design Tool for Estimating Passenger Ride Discomfort Within Complex Ride Environments. *Hum. Factors,* vol. 22, no. 3, June 1980, pp. 291–312.
6. Leatherwood, Jack D.; Clevenson, Sherman A.; and Hollenbaugh, Daniel D.: Evaluation of Ride Quality Prediction Methods for Operational Military Helicopters. *J. American Helicopter Soc.* vol. 29, no. 3, July 1984, pp. 11–18.
7. Leatherwood, Jack D.; and Barker, Linda M.: *A User-Oriented and Computerized Model for Estimating Vehicle Ride Quality.* NASA TP-2299, 1984.
8. Davis, Donald J.; Linse, Dennis J.; Suikat, Reiner; and Entz, David P.: *Preliminary Control Law and Hardware Designs for a Ride Quality Augmentation System for Commuter Aircraft.* NASA CR-4014, 1986.
9. Wykes, John H.; and Borland, Christopher J.: B-1 Ride Control. *Active Controls in Aircraft Design,* AGARD-AG-234, Nov. 1978, pp. 11-1–11-15.
10. Phillips, William H.; and Kraft, Christopher C., Jr.: *Theoretical Study of Some Methods for Increasing the Smoothness of Flight Through Rough Air.* NACA TN 2416, 1951.

Table I. Physical Characteristics of Airplane

Overall dimensions:	
Span, ft	39.86
Length, ft	36.07
Height, ft	11.66
Weights:	
Empty, lb	3873
Maximum takeoff, lb	6300
Maximum landing, lb	6200
Powerplants:	
Type	Reciprocating, six cylinder, horizontally opposed
Fuel system	Fuel-injected
Aspiration	Turbocharged
Rated power (at 2700 rpm and 34.5 in. Hg MAP), hp	300 (each)
Normal operating speed, rpm	2100 to 2450
Propeller type	3 blades
Propeller diameter, in.	76.5
Propeller control	Constant speed, full feathering
Wing:	
Area, ft^2	195.7
Mean aerodynamic chord, in.	61.99
Aspect ratio	8.1
Maximum wing loading, lb/ft^2	32.2
Center-of-gravity limits (at maximum takeoff weight):	
Forward, percent of mean aerodynamic chord	18.8
Aft, percent of mean aerodynamic chord	33.2

Table II. Flight Test Conditions

Condition	Altitude, ft	Indicated airspeed, knots	Engine speed, rpm	MAP, in. of Hg
Taxi	0		800	17.0
Engine run-up	0	0	1700	19.0
Takeoff roll	0	0 to 90	2700	34.5
Maximum climb	5000	110	2700	34.5
Cruise climb	5000	125	2450	29.5
Cruise	7500	155	2300	29.0
Descent	5000	150	2300	22.0
Landing roll	0	≈75 to 0		Idle

Table III. Typical Ride Quality Meter Printout

```
TIME = 90:36

63 Hz = 69.0710
DN = 00.9665

125 Hz = 93.6855
DN = 03.6694

250 Hz = 77.5430
DN = 01.1518

500 Hz = 79.8982
DN = 01.1017

1 kHz = 76.4843
DN = 00.9296

2 kHz = 69.3497
DN = 00.9520

DTOTAL = 05.0873
DVIB = 00.9213
DNOISE = 04.1661

DLONG = 00.0082
GLONG = 00.0006

DPITCH = 00.0792
GPITCH = 00.0091

DROLL = 00.3260
GROLL = 00.1189

DLAT = 00.2475
GLAT = 00.0028

DVERT = 00.6951
GVERT = 00.0102
```

Legend

TIME	Elapsed time in minutes and seconds since RQM power on
__Hz	Center frequency of octave band for which numerical value of A-weighted sound pressure level is given in decibels
DN	Noise discomfort index (without acceleration), DISC units
DTOTAL	Total discomfort index, DISC units
DVIB	Combined-axes acceleration discomfort index, DISC units
DNOISE	Combined noise discomfort index, DISC units
DLONG, DPITCH, DROLL, DLAT, DVERT	Single-axis acceleration Discomfort indexes, DISC units
GLONG, GLAT, GVERT	Frequency-weighted RMS linear acceleration, *g* units
GPITCH, GROLL	Frequency-weighted RMS angular acceleration, rad/sec^2

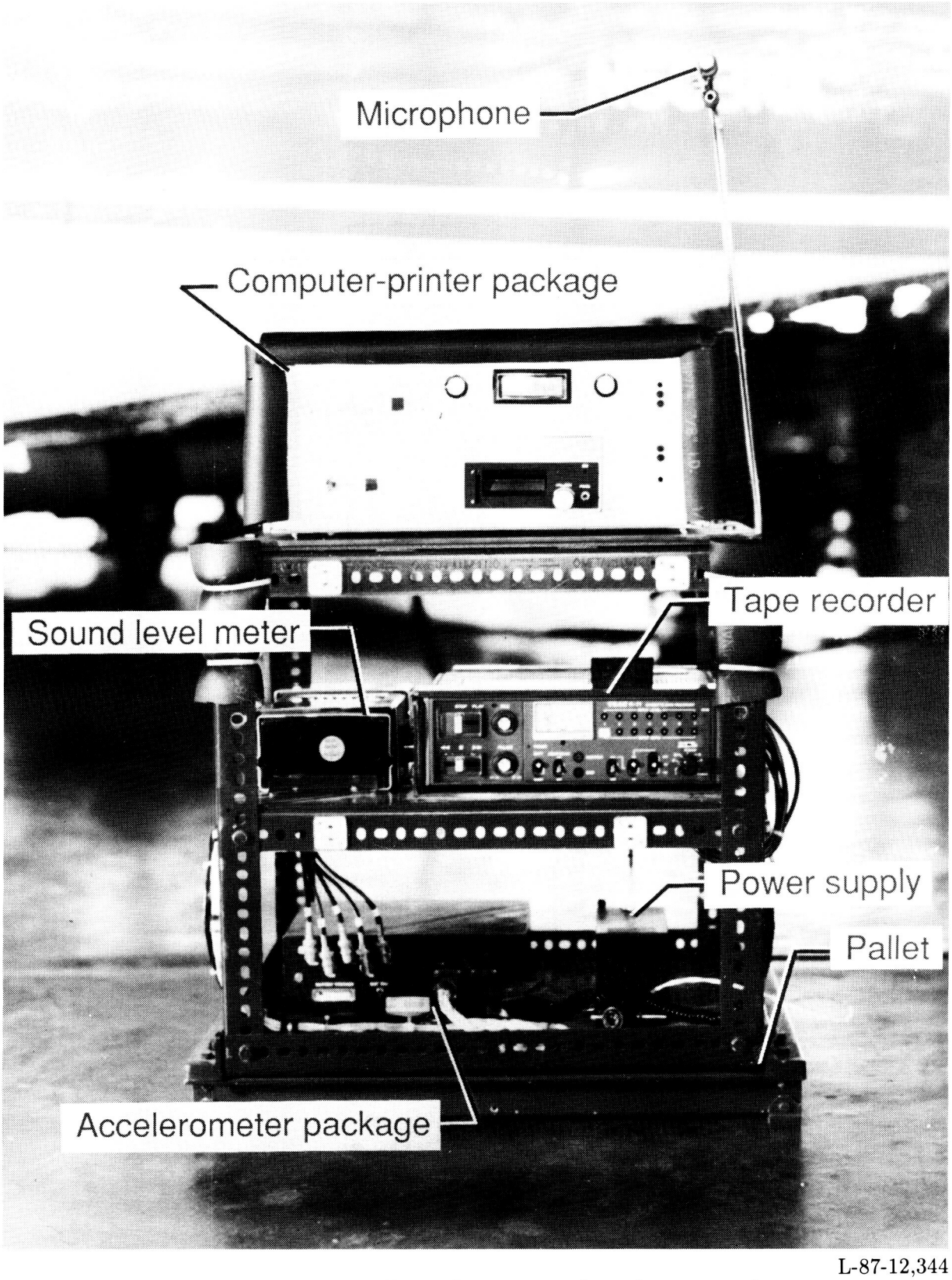

L-87-12,344

Figure 1. RQM on pallet with power supply and tape recorder.

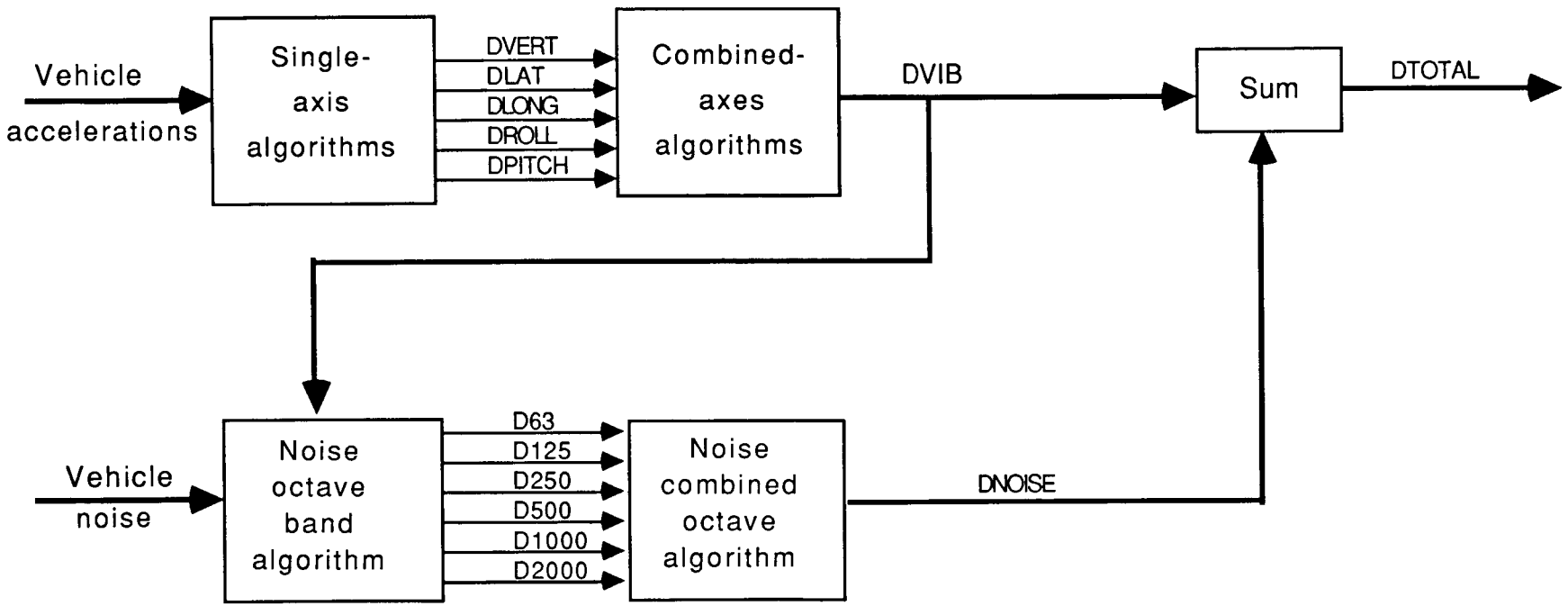

Figure 2. Elements of ride quality math model.

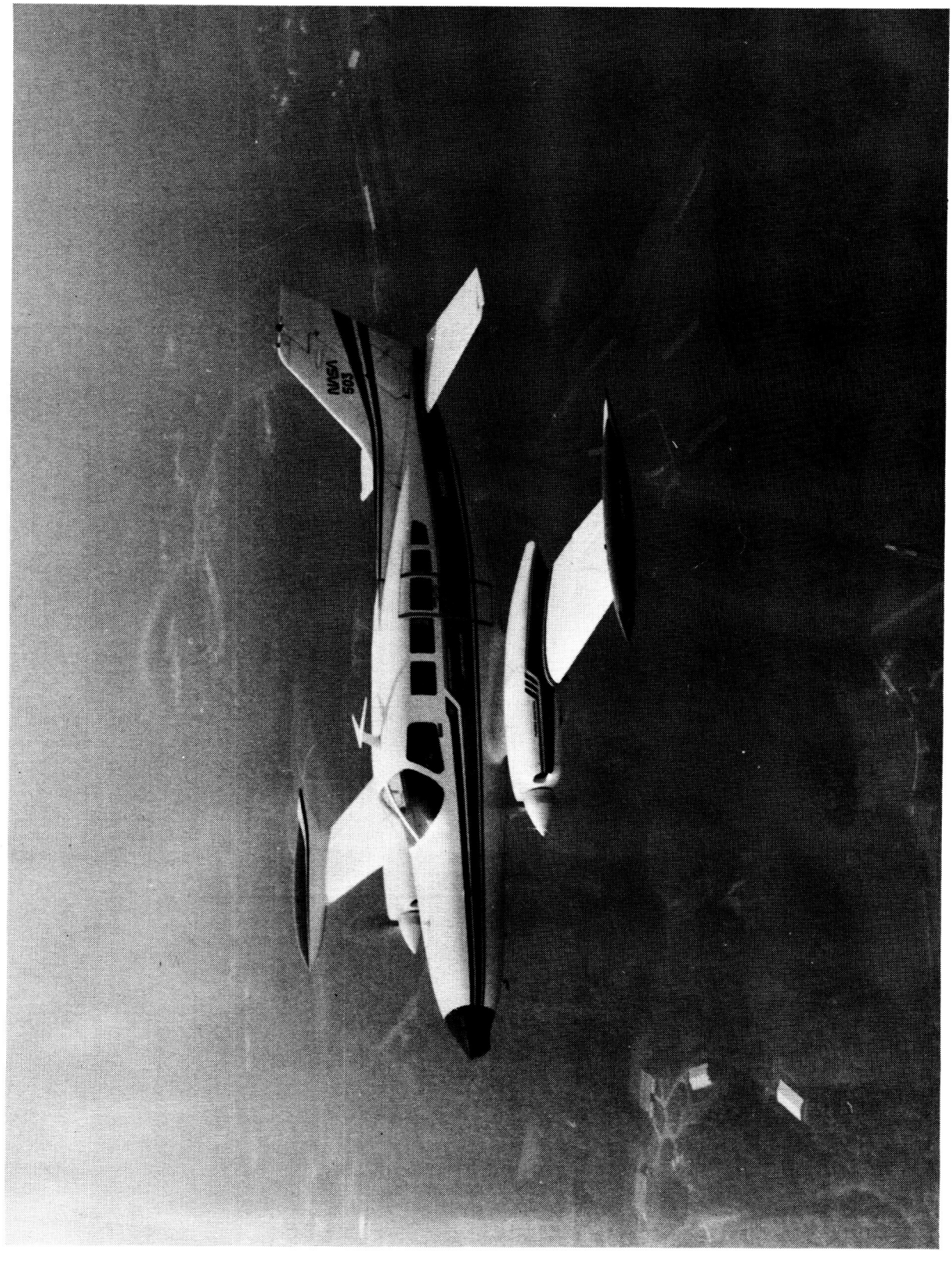

L-82-10,155

Figure 3. Test airplane.

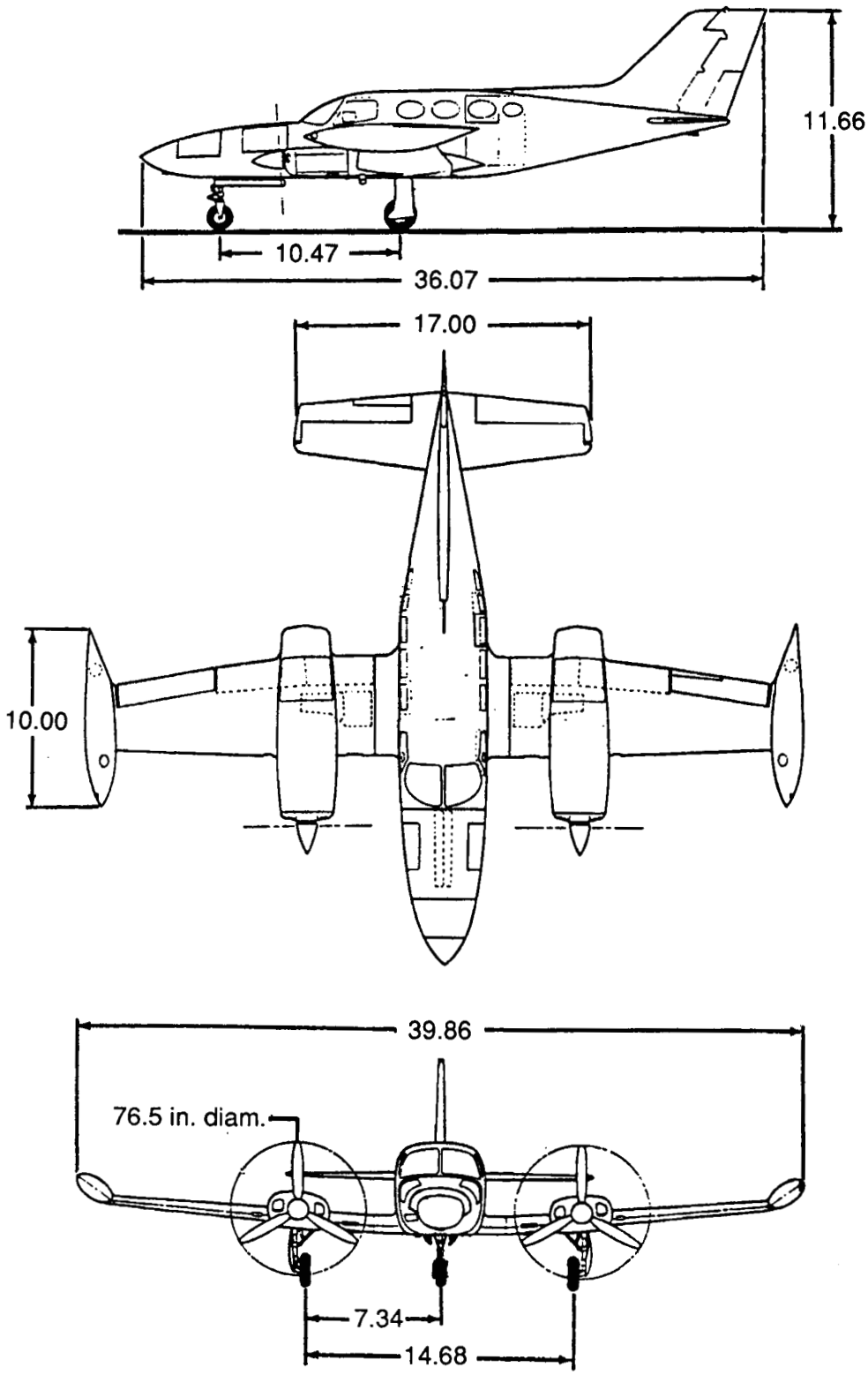

Figure 4. Drawing of test airplane. Dimensions are in feet unless noted otherwise.

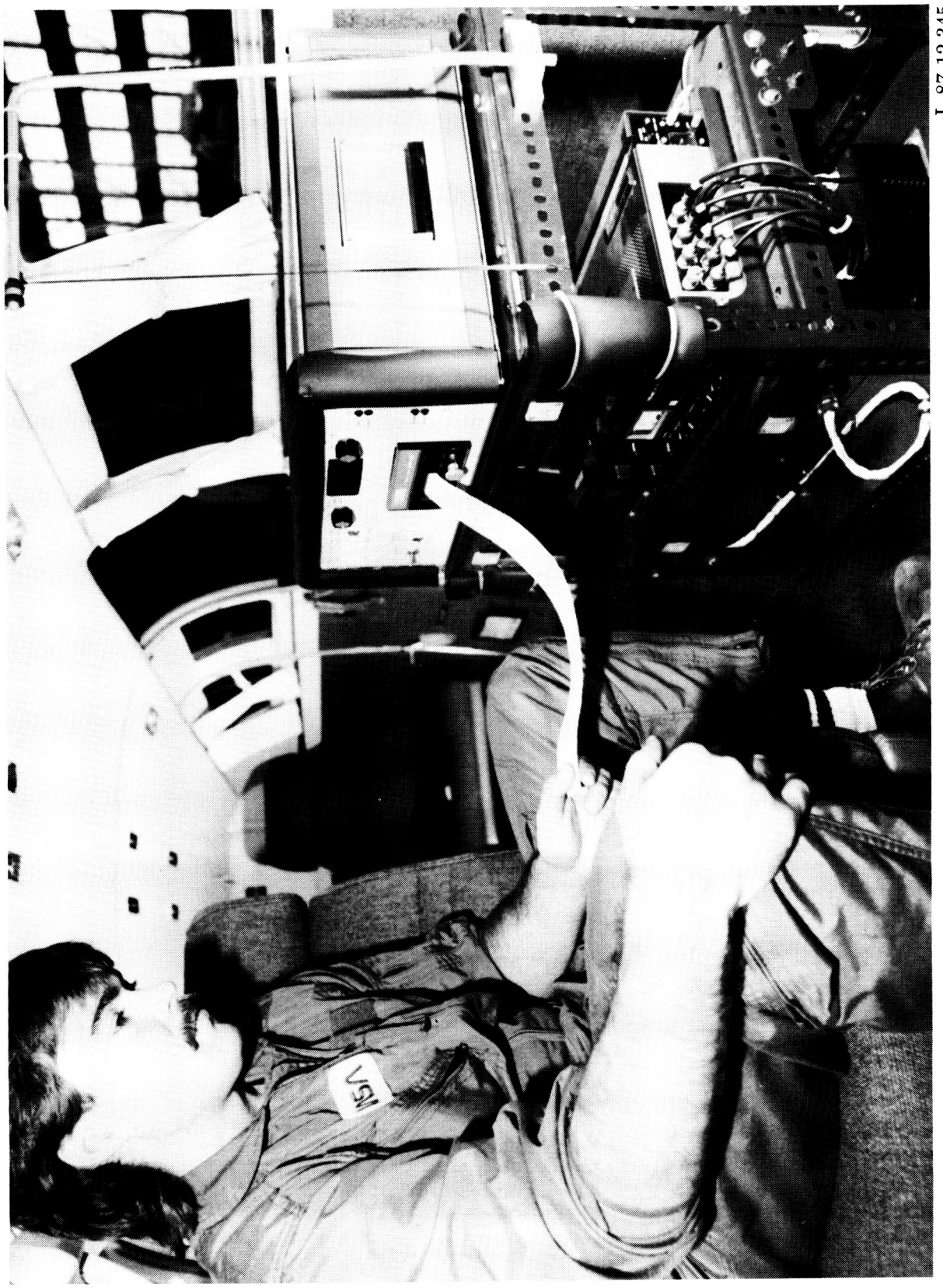

L-87-12,345

Figure 5. Experimental installation of RQM in test airplane.

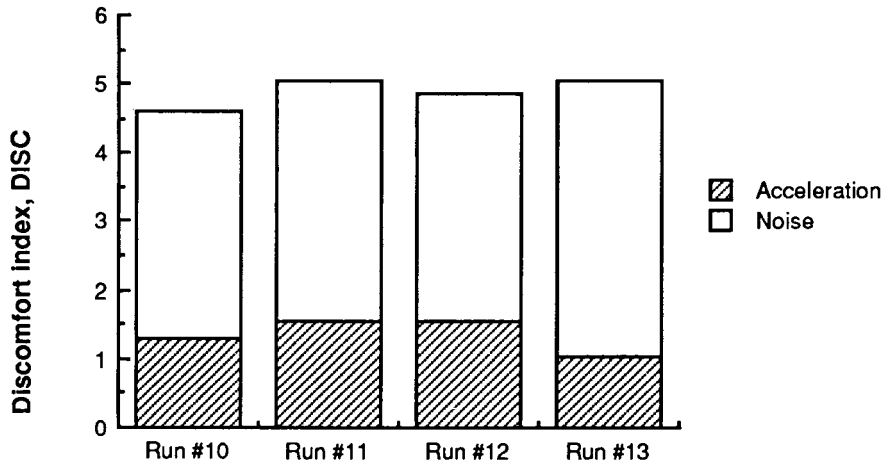

Figure 6. Repeat discomfort readings at cruise flight condition in very light turbulence.

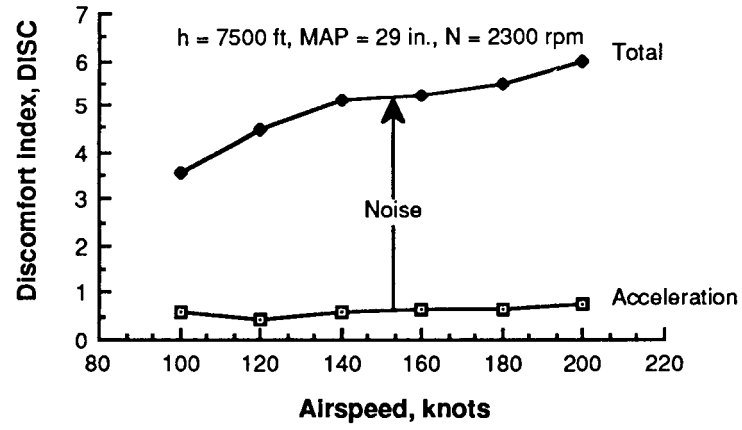

Figure 7. Effect of airspeed on discomfort index in smooth air.

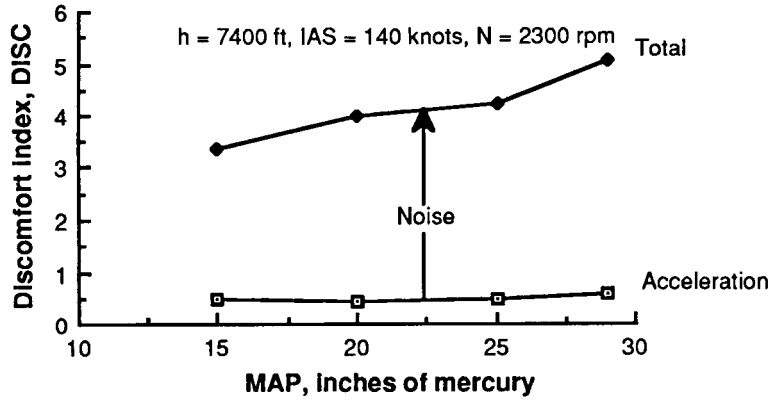

Figure 8. Effect of engine power on discomfort index in smooth air.

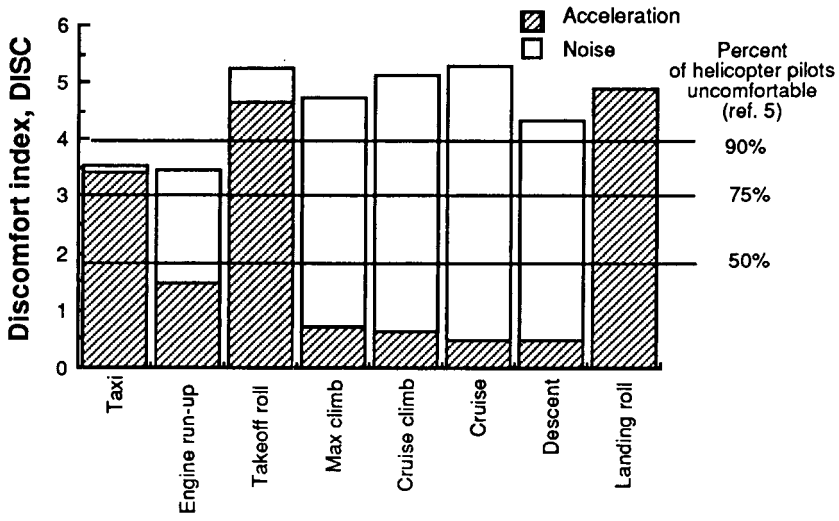

Figure 9. Discomfort indexes for different phases of flight in smooth air.

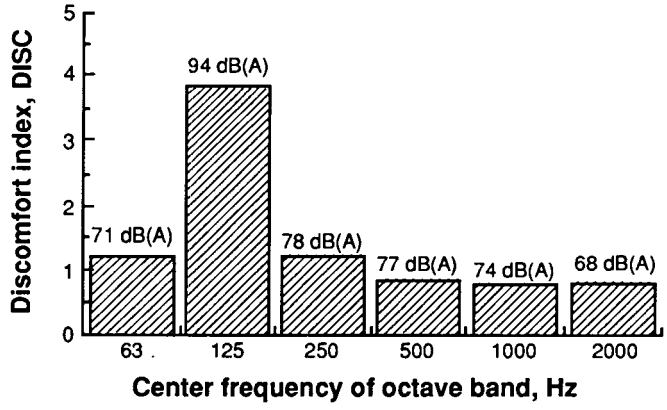

Figure 10. Components of noise discomfort at cruise in smooth air, uncorrected for accelerations.

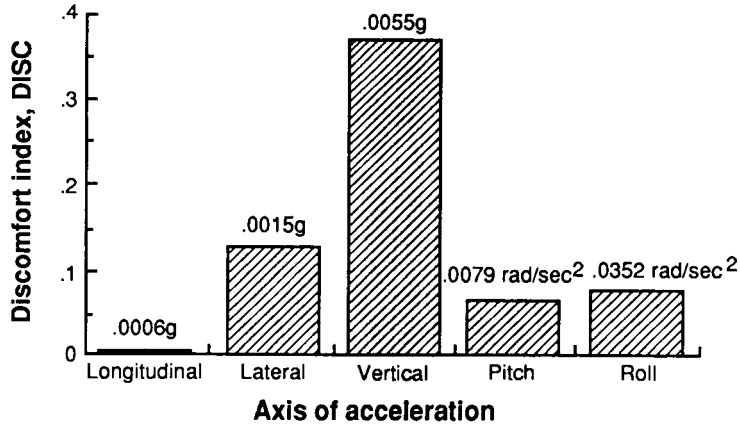

Figure 11. Components of acceleration discomfort at cruise in smooth air. Values given above bars are the weighted rms accelerations.

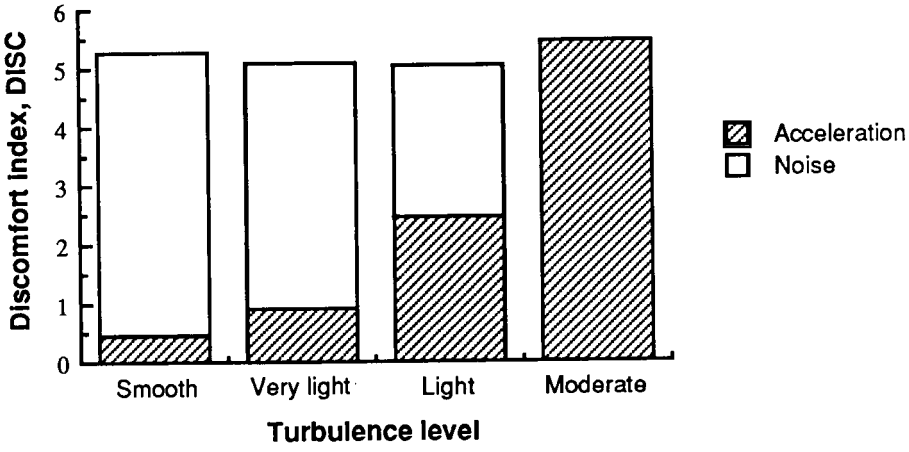

Figure 12. Ride quality indexes for different levels of turbulence.

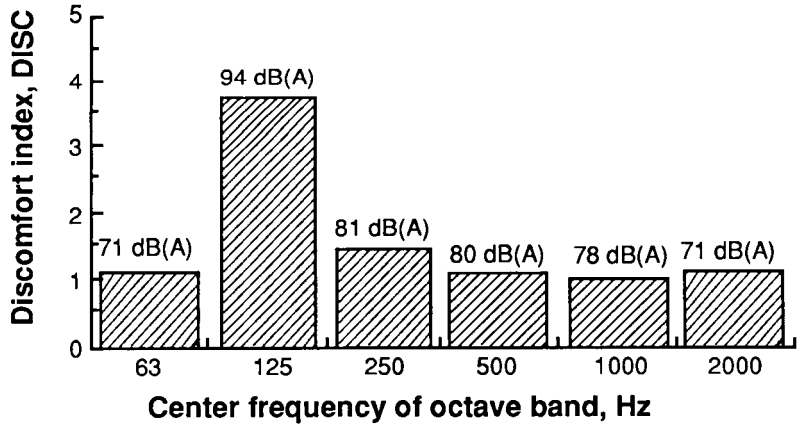

Figure 13. Components of noise discomfort in moderate turbulence, uncorrected for accelerations.

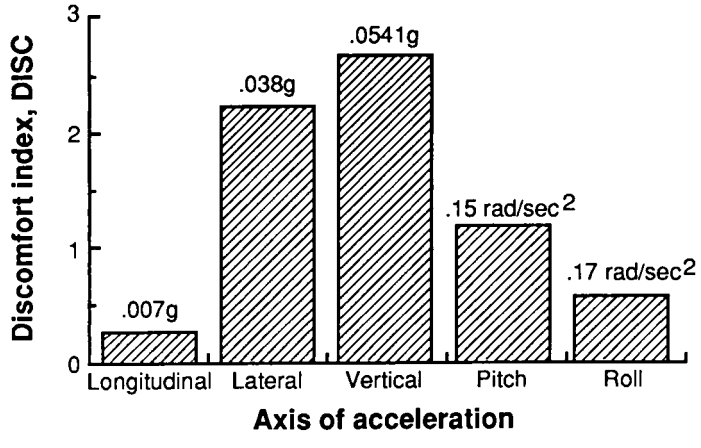

Figure 14. Components of acceleration discomfort at cruise in moderate turbulence. Values given above bars are the weighted rms accelerations.

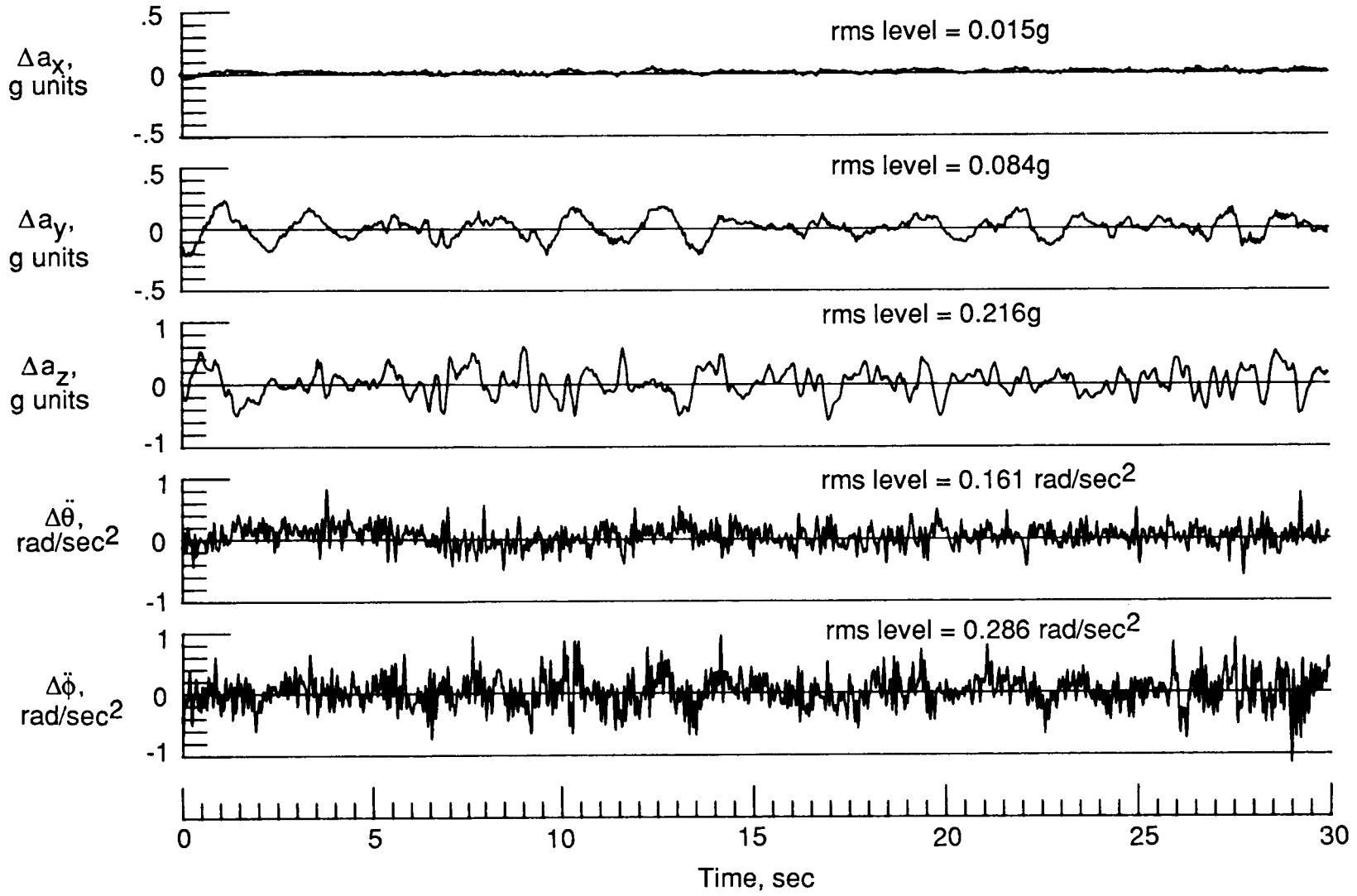

Figure 15. Acceleration time histories in moderate turbulence.

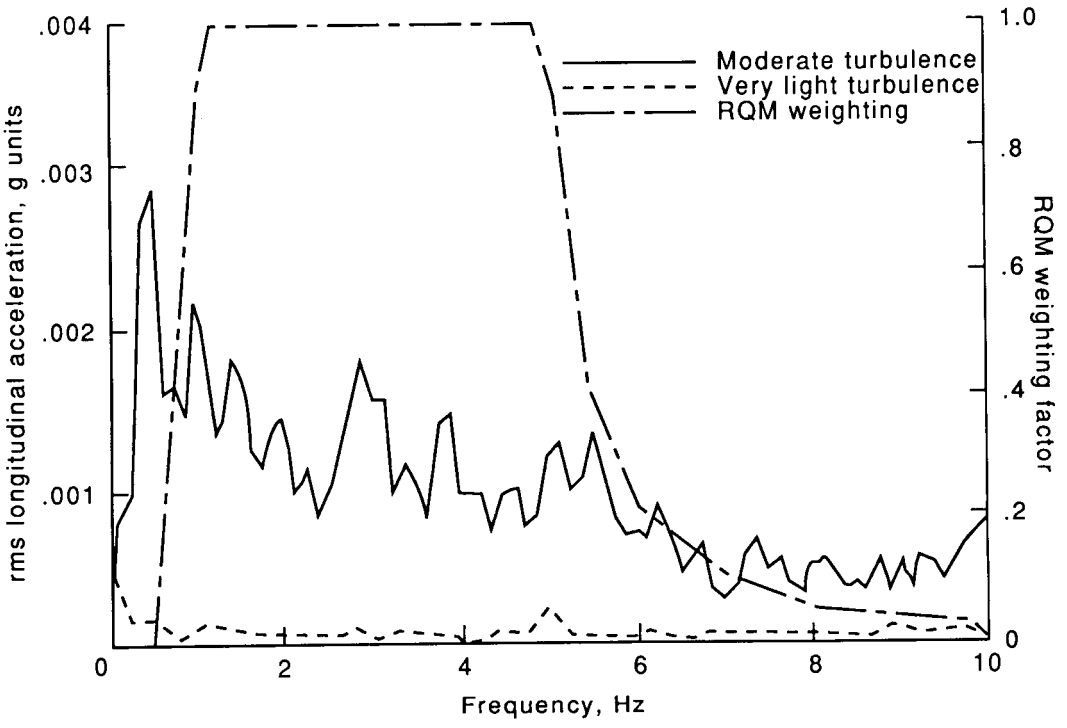

Figure 16. Longitudinal acceleration rms spectra (frequency resolution = 0.125 Hz) and RQM frequency weighting.

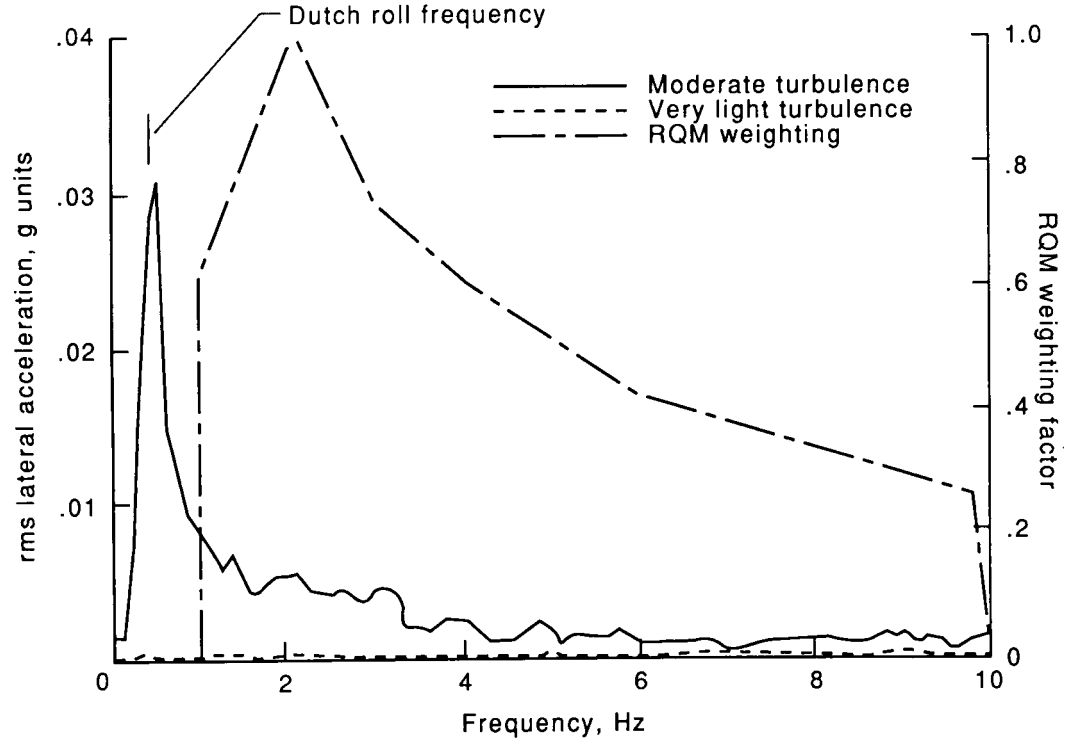

Figure 17. Lateral acceleration rms spectra (frequency resolution = 0.125 Hz) and RQM frequency weighting.

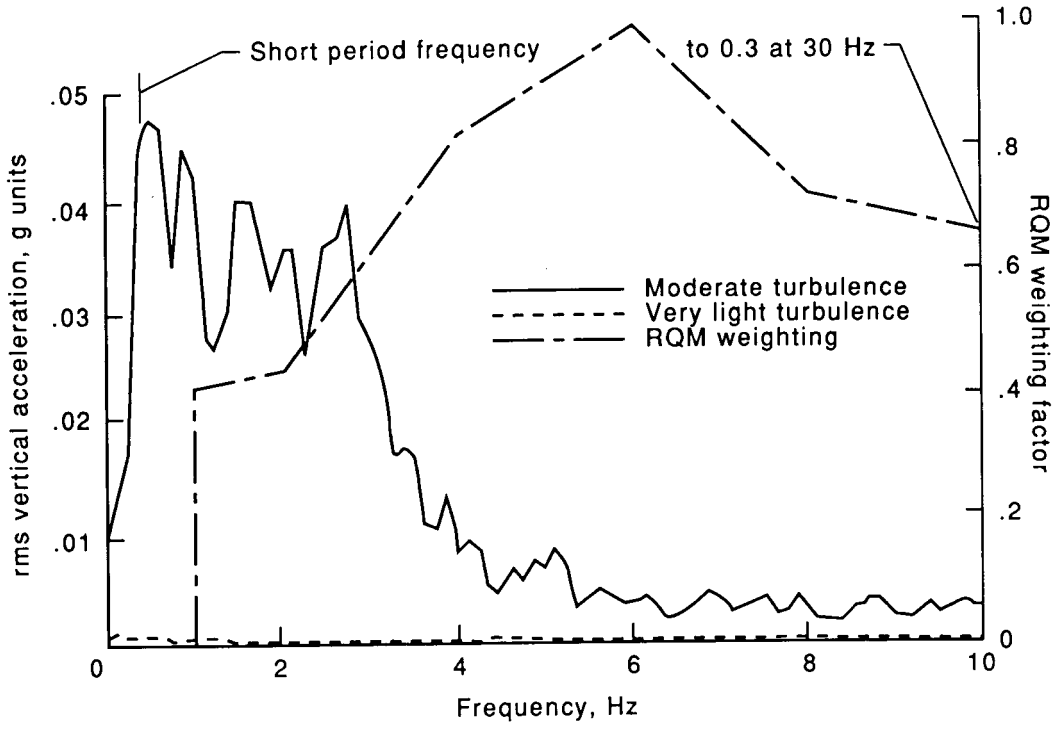

Figure 18. Vertical acceleration rms spectra (frequency resolution = 0.125 Hz) and RQM frequency weighting.

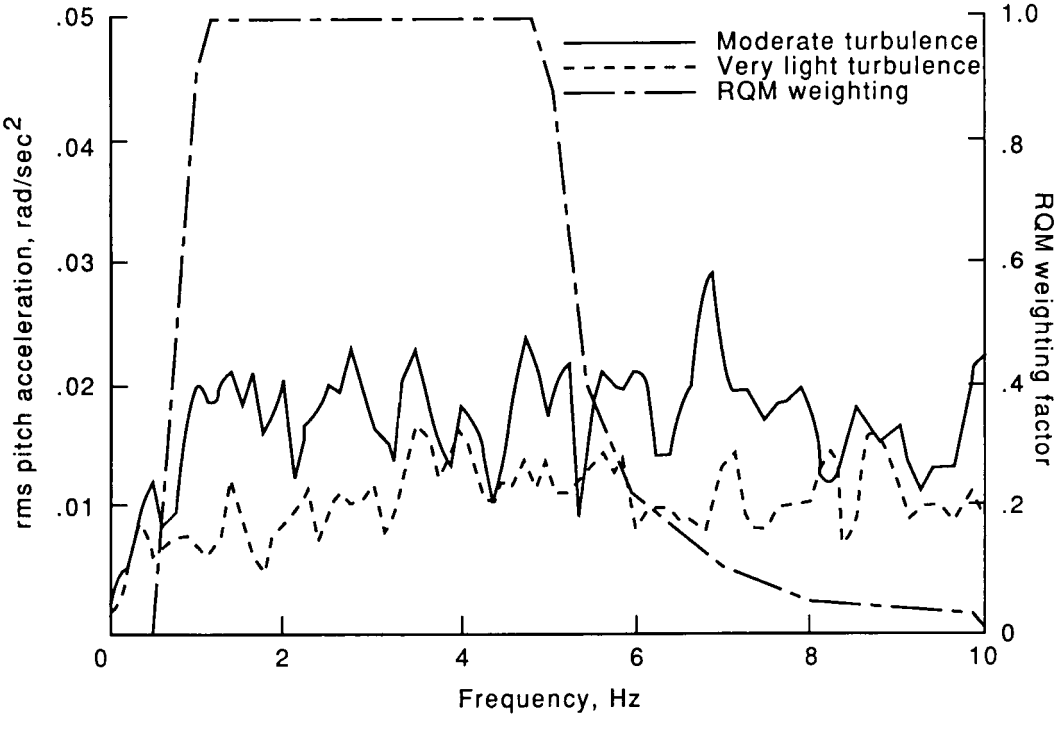

Figure 19. Pitch acceleration rms spectra (frequency resolution = 0.125 Hz) and RQM frequency weighting.

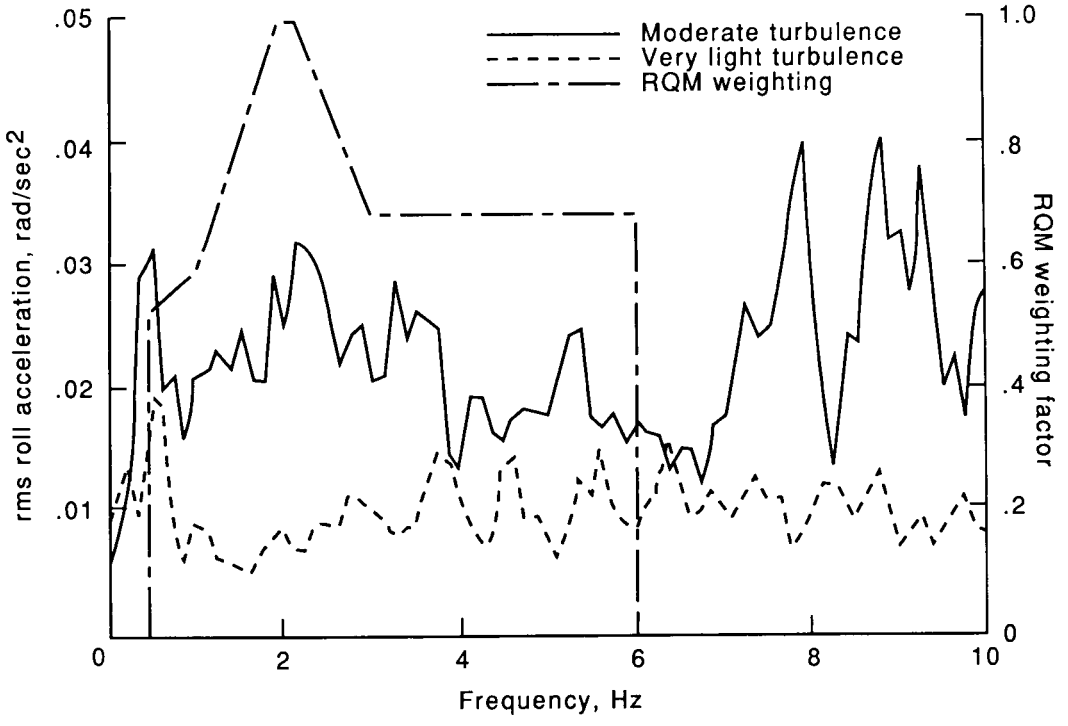

Figure 20. Roll acceleration rms spectra (frequency resolution = 0.125 Hz) and RQM frequency weighting.

NASA
National Aeronautics and Space Administration

Report Documentation Page

1. Report No.	2. Government Accession No.	3. Recipient's Catalog No.
NASA TP-2913		

4. Title and Subtitle	5. Report Date
Evaluation of the Ride Quality of a Light Twin-Engine Airplane by Means of a Ride Quality Meter	June 1989
	6. Performing Organization Code
7. Author(s)	8. Performing Organization Report No.
Eric C. Stewart	L-16524
9. Performing Organization Name and Address	10. Work Unit No.
NASA Langley Research Center Hampton, VA 23665-5225	505-61-41-02
	11. Contract or Grant No.
12. Sponsoring Agency Name and Address	13. Type of Report and Period Covered
National Aeronautics and Space Administration Washington, DC 20546-0001	Technical Paper
	14. Sponsoring Agency Code

15. Supplementary Notes

16. Abstract

A ride quality meter has been used to establish the baseline ride quality of a light twin-engine airplane planned for use as a test bed for an experimental gust alleviation system. The ride quality meter provides estimates of passenger ride discomfort as a function of cabin noise and vibration (acceleration) in five axes (yaw axis omitted). According to the ride quality meter, in smooth air the cabin noise was the dominant source of passenger discomfort. In moderately turbulent air with approximately the same cabin noise level, the vertical and lateral vibrations (accelerations) were the dominant sources of passenger discomfort, but the total discomfort was approximately the same as that for the smooth-air condition. The researcher's subjective opinion, however, is that the total ride discomfort was much worse in the moderate turbulence than it was in the smooth air. The discrepancy is explained by the lack of measurement of the low-frequency accelerations by the ride quality meter.

17. Key Words (Suggested by Authors(s))	18. Distribution Statement
Light airplanes Ride quality Cabin noise Vibration Turbulence	Unclassified—Unlimited Subject Category 01

19. Security Classif. (of this report)	20. Security Classif. (of this page)	21. No. of Pages	22. Price
Unclassified	Unclassified	25	A03

For sale by the National Technical Information Service, Springfield, Virginia 22161-2171